CONFERENCE PRE-PRINT

n=0 VERTICAL DISPLACEMENTS, IMPACT OF MAGNETIC X-POINTS, AND VERTICAL DISPLACEMENT OSCILLATORY MODES DRIVEN BY FAST IONS IN TOKAMAK PLASMAS

¹F. PORCELLI, ¹D. BANERJEE, ¹S. CAVALLERO, ²T. BARBERIS, ³F. QIU, ³A. YOLBARSOP, ⁴L.-G. ERIKSSON, ⁵C.C. KIM.

Department of Applied Science and Technology, Polytechnic University of Turin, Torino, Italy

²Princeton Plasma Physics Laboratory, Princeton, NJ, USA

³Department of Plasma Physics and Fusion Eng., University of Science and Technology of China, Hefei, China

⁴Department of Space, Earth and Environment, Chalmers University of Technology, Gothenburg, Sweden

⁵SLS2 Consulting, San Diego, California, USA

Email: francesco.porcelli@polito.it

Abstract

Recent progress on the theory, numerical simulations, and experimental observations of Vertical Displacement Oscillatory Modes (VDOM) in tokamak experiments is reported. VDOM are driven unstable by energetic particles and can have an impact on plasma disruptions, plasma edge stability and confinement. These modes are a candidate to explain Alfvénfrequency n=0 modes recently observed on JET, TCV, and MAST-U. The specific types of fast ion distribution functions that can provide an instability drive for VDOM are discussed. Numerical results obtained by the NIMROD code regarding the simulation of n=0 modes driven by fast ions are shown.

1. INTRODUCTION

A new type of fast ion driven instability involving axisymmetric modes (toroidal mode number n=0) in magnetically confined tokamak plasmas was discovered recently [1]. The relevant mode has been dubbed Vertical Displacement Oscillatory Mode (VDOM). The linear dispersion relation for this mode was obtained analytically in [1-4]. An estimate of the linear threshold for the destabilization of this mode in terms of critical fast ion density was discussed in [1]. VDOM oscillate with a relatively high frequency, of the order of the Alfvén frequency based on the poloidal magnetic field. High-frequency n=0 modes have been observed in recent JET discharges, see e.g. Fig. 3 of Ref. [5] and Fig. 12 of Ref. [6]. Alpha particle driven n=0 modes have been clearly identified during the last DT3 campaign on JET [7, 8]. n=0 modes driven by NBI fast ions have been observed on TCV and on MAST-U [9]. Simple extrapolations and numerical simulations suggest that these modes are likely to be observed also in future tokamak experiments such as JT-60SA, SPARC, BEST, DTT, and ITER. Since the VDOM instability relies on gradients of the fast ion distribution in velocity space, unstable VDOM may lead to a faster relaxation of fusion alpha particles in velocity space, rather than alpha particle radial transport and loss of confinement. In this sense, unstable VDOM should not pose a real danger for alpha particle confinement in fusion burning plasmas. Nevertheless, since VDOM are global in nature and can affect the edge plasma region through the production of current sheets in the vicinity of magnetic X-points of the divertor separatrix [10], they may give rise to an important coupling between the plasma core, where the fast particle drive is dominant, and the plasma edge, with consequences on the stability of ELMs and an impact on the plasma dynamics in the divertor region. It has been conjectured that VDOM may nonlinearly destabilize low-frequency vertical displacements, acting as a trigger for Vertical Displacement Events (VDE) and disruptions. These considerations motivate further studies of n=0 modes. In this article, our main objective is to review the recent progress in the understanding of VDOM. Nevertheless, this article will also contain some original work, namely: (i) A discussion (Sec. 3) on the limits of plasma elongation for stable operation against the vertical instability in the ideal-MHD limit; (ii) Specific types of fast ion distributions giving rise to a positive drive for n=0 modes (Sec. 5); (iii) New advances on the numerical simulation of n=0 modes in realistic tokamak geometry taking into account the fast ion drive (Sec. 6).

2. A SHORT REVIEW OF THE ANALYTIC THEORY OF VERTICAL DISPLACEMENT OSCILLATORY MODES

There are four different types of n=0 modes that are relevant for tokamak plasmas: (i) Global Acoustic Modes (GAM) [11], which oscillate with a relatively low frequency of the order of the sound wave frequency; Global Alfvén Eigenmodes (GAE) [12] (GAE); Vertical Displacement Oscillatory Modes (VDOM) [2]; Zero-frequency Vertical Displacements (VD) [13], which can lead to VDE and disruptions. While the theory of GAM, GAE and

VD is well developed, VDOM is a relatively new entry. For this reason, this article will be concerned mainly with the theory and numerical simulations of VDOM.

GAE and VDOM oscillate with a frequency of the order of the poloidal Alfvén frequency. They are both largely immune to continuum damping. Thus, they are both good candidates to explain the recent experimental observations of n=0 modes mentioned in the Introduction. However, they have different mode structures, and the mechanisms underlying GAE and VDOM are also different. The GAE exists as a shear Alfvén mode that avoids continuum damping due to a minimum in the $k_{\parallel}v_A$ spectrum. Normally, the GAE mode structure undergoes a rapid variation near the plasma edge, where the minimum of $k_{\parallel}v_A$ as function of radius occurs, because the safety factor (q) and the plasma density tend to vary quickly in that region. Thus, GAEs are sensitive to details of q and of plasma density [12]. By contrast, VDOMs are external modes interacting with currents induced on the nearby first wall, under conditions of passive wall stabilization of the ideal-MHD vertical instability. The resulting electromagnetic forces, coupling the plasma current and the induced wall currents, oppose further vertical movements, causing a global vertical oscillation of the entire plasma column [2].

VDOM and VD are intimately related. A dispersion relation that can treat both VDOM and VD was obtained analytically in Ref. [2], based on the reduced ideal-MHD model (in the absence of fast ions) and on a simplified straight-tokamak equilibrium [14] assuming a constant q profile (so to exclude *a priori* the presence of GAE), with the plasma bounded by an elliptical flux surface (with a and b the minor and major semi-axes). The plasma is confined within a resistive wall, which is also taken to be ellipse with semi-axes a_w and b_w . Confocality is assumed: $b_w^2 - a_w^2 = b^2 - a^2$. The dispersion relation is cubic in the complex eigenfrequency $\gamma = -i\omega$:

$$\gamma^3 + \frac{\gamma^2}{(1-\hat{e}_0)\tau_\eta} + \gamma\omega_0^2 + \frac{\omega_0^2}{(1-D)\tau_\eta} = 0 \tag{1}$$

where τ_{η} is the resistive wall time, $e_0 = (b^2 - a^2)/(b^2 + a^2)$ is the ellipticity parameter, $\hat{e}_0 = \kappa/(1 + \kappa)$, $\kappa = b/a > 1$ is the plasma elongation, $D = D(\kappa, b/b_w)$ is a geometric wall parameter,

$$\omega_0 = \left(\frac{D-1}{1-\hat{e}_0}\right)^{1/2} \gamma_{\infty}, \text{ where } \gamma_{\infty} = \frac{2\kappa}{1+\kappa^2} \left(\frac{\kappa-1}{k}\right)^{1/2} \tau_A^{-1} \text{ and } \tau_A = \frac{B_p'}{(4\pi\varrho_m)^{1/2}}.$$
 (2)

In this dispersion relation, τ_A is the poloidal Alfvén time and γ_∞ is the ideal-MHD VD growth rate found in the no-wall limit, $b/b_w \to 0$, such that also $D \to 0$ (see the next Section for a definition and a more detailed discussion of the parameter D). When D < 1, VDs are ideal-MHD unstable, growing on the Alfvén time scale, i.e., a few micro-seconds for typical tokamak parameters. It would be impossible to prevent the rapid growth of a VDE in that limit. Passive-wall stabilization of the ideal-MHD VD requires $D \ge 1$. When this inequality is satisfied, ω_0 is a real (positive) quantity. For values of D not very close to unity, such that $\omega_0 \sim \tau_A^{-1}$, the relevant regime is $\omega_0 \tau_\eta \gg 1$. In that limit, the three roots of dispersion relation (1) are

$$\omega = \pm \omega_0 - i \frac{(1 - \hat{e}_0)D}{2(D - 1)(1 - \hat{e}_0D)\tau_\eta}; \qquad \gamma = \frac{1}{(D - 1)\tau_\eta}.$$
 (3)

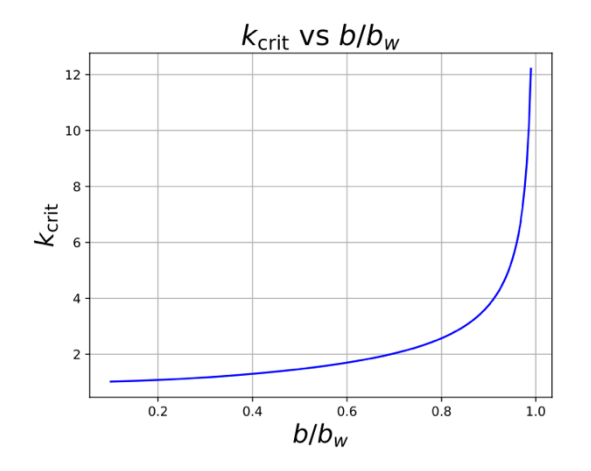
The first two roots in Eq. (3) correspond to VDOM oscillating with a frequency $\Re(\omega) = \pm \omega_0$ (\Re stand for "real part"). As we can see from this equation, the VDOM are normally stable normal modes with a damping rate related to the wall resistivity. However, VDOM can be driven unstable by fast particles, as discussed in Sec. 5. The third, zero-frequency root correspond to a n=0 VD slowly growing on the resistive wall time scale, i.e., a few milli-seconds for typical tokamak parameters. Since in this regime the VD grows slowly, it can be completely suppressed by active feedback stabilization. We observe, however, that close to ideal-MHD marginal stability, i.e., when D is close to unity and the condition $\omega_0 \tau_\eta \gg 1$ is not satisfied, the resistive VD can grow much more rapidly, with a growth rate scaling with a fractional power of wall resistivity [3]. In this regime, the active feedback stabilization system would no longer be capable of preventing the growth of a VD leading to a VDE.

3. HOW MUCH ELONGATION IS TOO MUCH ELONGATION?

Let us discuss in more details the criterion $D \ge 1$ for the stabilization of the ideal-MHD VD. For the analytic model introduced in Ref [2, 15] (see also [16]), an expression for the geometric wall parameter is

$$D(\kappa, b/b_w) = \frac{\kappa^2 + 1}{(\kappa - 1)^2} \left\{ 1 - \left[1 - \frac{\kappa^2 - 1}{\kappa^2} \left(\frac{b}{b_w} \right)^2 \right]^{1/2} \right\}$$
 (4)

As pointed out in Sec. 2, this expression assumes confocal ellipses for the plasma boundary and the plasma wall. It is, therefore, a rather crude approximation of the actual tokamak equilibrium configuration. X-points in a double-null configuration, lying on a divertor separatrix, are allowed by this approximation [14]. However, the hot plasma is assumed to extend to an elliptical boundary and not to the magnetic separatrix, so that the X-points lie either in vacuum or in a cold, halo plasma region (we shall discuss in the next section the consequences of relaxing this assumption). Also, in a real tokamak experiment, plasma-facing components are often placed inside the vacuum chamber to ensure passive wall stabilization of the ideal-MHD vertical instability. Bearing in mind all these caveats, we may still use Eq. (4) to discuss a very relevant question: are there limits on plasma elongation, such that, for $\kappa > \kappa_{crit}$, D falls below unity and vertical displacements become ideal-MHD unstable?



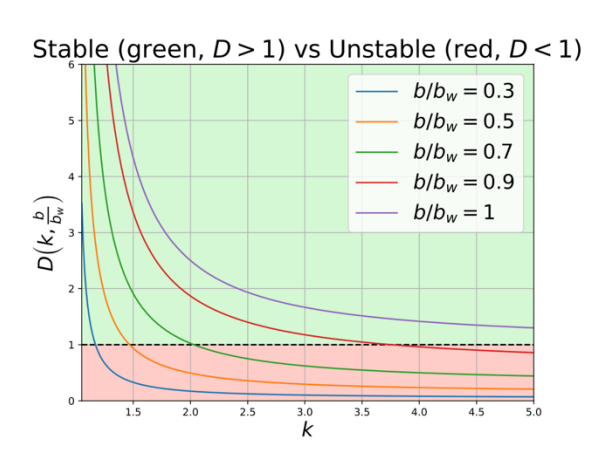


Fig. 1: Critical elongation, κ_{crit} , vs normalized plasmawall distance, b/b_w . When the plasma touches the wall, $b/b_w = I$.

Fig. 2: The geometric wall parameter $D(\kappa, b/b_w)$ vs elongation κ for different values of the normalized plasmawall distance, b/b_w .

The short answer to this question is: no, there are no limits on plasma elongation, if the wall can be placed sufficiently close to the plasma boundary. This is illustrated by Fig. 1, where we set $D(\kappa_{crit}, b/b_w) = 1$ and we solved for κ_{crit} as function of b/b_w . As one can see from this figure, $\kappa_{crit} \to \infty$ when the plasma touches the wall, $b/b_w=1$. However, some distance must always be allowed between the plasma and the wall. Therefore, in practical terms, a critical elongation does exist. In Fig. 2, we show D as function of κ for different values of b/b_w . The stable domain corresponds to the green region, where D > 1. One can see that for values of b/b_w between 0.7 and 0.9, the critical elongation can vary significantly, from $\kappa_{crit} = 2$ to $\kappa_{crit} = 3.7$.

As discussed in [3], another important consequence of confocality between the elliptical plasma boundary and the elliptical wall is that the marginal stability condition, D=1, corresponds to the situation where the wall intercepts the X-points. Ideal-MHD stability requires the X-points to lie outside the vacuum chamber. When comparing with realistic tokamak equilibria, this criterion appears to be somewhat restrictive, as the actual wall in a tokamak experiment is closer on average to the plasma than the confocal wall assumed in analytic work. Furthermore, single-null divertor configurations normally have one magnetic X-point inside the vacuum chamber and a second one outside. Thus, numerical work with more accurate plasma equilibria and wall geometry is required. However, it appears from this analysis that, for a double-null divertor configuration where both magnetic X-points lie inside the vacuum chamber, considering the actual wall geometry, the ideal-MHD stability criterion can at best only marginally be satisfied, which motivates the use of plasma-facing coils inside the vacuum chamber to help guarantee passive wall stabilization.

The idealized equilibrium [14] used in Refs. [2, 3, 15] and in this article, leading to the Eq. (4) for the geometric wall parameter D and to the criterion $D \ge 1$ for ideal-MHD stability of vertical displacement, is the same equilibrium used in the pioneering work by Laval et al [16]. If expressed in terms of κ and $\kappa_w = b_w/a_w$, and keeping in mind the confocality condition, $b_w^2 - a_w^2 = b^2 - a^2$, the criterion $D \ge 1$ becomes

$$D = \frac{\kappa^2 + 1}{(\kappa - 1)^2} \frac{\kappa_W - 1}{\kappa_W} \ge 1,\tag{5}$$

which is consistent with Ref. [16], but corrects a misprint in the widely used book *Tokamaks*, by J. Wesson (see Eq. (6.15.1) of Ref. [17]).

4. IMPACT OF MAGNETIC X-POINTS

The analysis of the previous two sections assumed that the magnetic X-points of the simplified, double-null equilibrium configuration used for analytic work lie either outside the vacuum chamber, or, if inside, they lie in vacuum or in a cold, low-density halo plasma region. In reality, for a realistic tokamak divertor configuration, the hot plasma extends to the magnetic separatrix (the last-closed-magnetic-surface), where the X-points are located. As discussed in Ref. [10] based on analytic considerations, and shown numerically in Refs. [18], the most likely consequence is that axisymmetric current sheets localized around the magnetic X-points and extending along the magnetic separatrix are driven by n=0 perturbation. In Ref. [10] it was concluded that these X-point current sheets, which become singular with a vanishing width in the ideal-MHD limit, can have a stabilizing effect on vertical plasma displacements. However, the theory of Ref. [10] lacks consideration of resistive effects, which can resolve the ideal-MHD singularity, providing a characteristic width for the X-point current sheets. This problem is as yet unresolved. It is nevertheless a very relevant issue, since these X-points current sheets can have a profound impact on plasma edge stability (e.g., on the stability of peeling-ballooning modes leading to ELMs); furthermore, they are likely associated with axisymmetric sheared flows, which can affect the turbulent transport of plasma particles and energy across the plasma edge and into the open field line region.

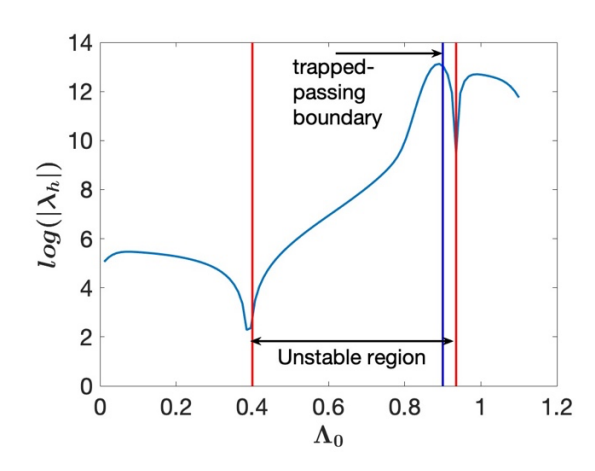
Magnetic X-points give rise to singularities in the ideal-MHD limit because the parallel wave-vector operator, $k_{\parallel} = \mathbf{b} \cdot \nabla$, where \mathbf{b} is the unit vector along the equilibrium magnetic field, vanishes identically for mode number n=0, since the poloidal component of the equilibrium magnetic field vanishes on the X-points. The resonance involves the toroidal field lines going through magnetic X-points. Because of this resonant, singular behavior, ideal-MHD becomes a poor representation of the plasma dynamics for axisymmetric perturbations in the vicinity of magnetic X-points. A better model involves dissipation and other extended-MHD effects, such as two-fluid effects, finite ion Larmor radius, and a generalized Ohm's law. Besides the mentioned analytic work [10], X-point current sheets have been observed in tokamak experiments [19, 20] and in numerical simulations [18, 21].

5. FAST PARTICLE DRIVE FOR VERTICAL DISPACEMENT OSCILLATORY MODES

GAM, GAE, and VDOM have in common that they can all be destabilized by their resonant interaction with fast ions, the relevant resonance condition is $\omega = p\omega_{t/b}$, where $\omega_{t/b}$ is the transit/bounce frequency of fast ions with passing/trapped orbits. GAM, being relatively low-frequency perturbations, can be destabilized by fast ions in the 50-100 keV range, arising, for instance, by Neutral Beam Injection; this energetic-particle-induced GAM, or EGAM, was first discussed in Ref. [11]. The drives for GAE [5] and for VDOM [1] require instead fast ions with energy ranging from several 100 keV to a few MeV. Nevertheless, the fast particle drives for all these modes have an important element in common: since n=0, the part of the perturbed fast ion distribution function that involves derivates of the equilibrium fast ion distribution, F_h with respect to the toroidal canonical momentum, $\partial F_h/\partial P_{\varphi}$, being multiplied by the toroidal mode number, is absent (see, e.g., Ref. [22]). Thus, a positive drive for n=0 requires bump-on-tail-like equilibrium distribution functions; more specifically, in at least some regions of phase space, a necessary condition for fast particle destabilization of n=0 modes is

$$\frac{\partial F_h}{\partial \varepsilon}\Big|_{\mu} = \frac{\partial F_h}{\partial \varepsilon}\Big|_{\Lambda} - \frac{\Lambda}{\varepsilon} \frac{\partial F_h}{\partial \Lambda}\Big|_{\varepsilon} > 0 \tag{6}$$

where $\mathcal{E} = mv^2/2$, $\mu = mv_\perp^2/2B$, and $\Lambda = \mu B_0/\mathcal{E}$, with B_0 the on-axis magnetic field. An isotropic distribution function in velocity space does not depend on the pitch angle variable, Λ . Thus, the standard, isotropic slowingdown distribution function for the fast ions, being monotonically decreasing as function of energy, does not satisfy Eq. (6). This may explain why n=0 saturated fluctuations are observed in tokamak experiments sometimes only transiently, for instance after sawtooth crashes [6, 23], or when NBI or ICRF heating is modulated or ramped up [6, 24], as a fully developed slowing down distribution requires time to form or be recreated, of the order of the slowing-down time. Two types of anisotropic fast ion distributions worth considering in this context are those created by Neutral Beam Injection (NBI) and acceleration of ions by ICRF waves. In large tokamaks, one must use very high injection energies for the beams to penetrate to the central regions of the plasma, in ITER typically one MeV, and at such energies the pitch angle scattering is very weak. Consequently, in the high energy range, the distribution function of injected ions will be narrow in the Λ direction and centred around the Λ_0 , the Λ value at the point of ionisation. For ions injected in the passing regions, focusing on VDOM and using the notations of Ref. [1], one can find approximate analytical expression for $|\Upsilon|^2$ and h_{Ω} . Armed with these and assuming a delta function distribution in the Λ direction, one finds analytically that the n=0 VDOM instability is driven for $\Lambda_0>$ 0.4 for ions injected into passing orbits. However, for ions injected in the trapped region the situation is significantly more complicated, as one can infer from the much stronger variation of both $|\Upsilon|^2$ and h_{Ω} in this region. This is illustrated in Fig. 3, which shows a full numerical evaluation of the normalised fast particle drive, λ'_h , (as defined in Ref. [25]) for ions injected with different Λ_0 . As expected, the instability is driven for $\Lambda_0 > 0.4$ in the passing region. It should be noted that the drive increases strongly as Λ_0 moves to the value corresponding to the trapped passing boundary. It is only near the trapped-passing boundary that the instability is driven for particles injected into trapped orbits. This is strongly linked to the peak of $|\Upsilon|^2$ in the trapped region.



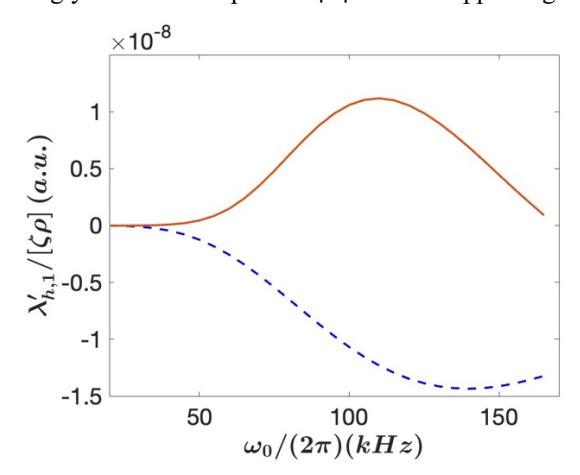


Fig. 3: Normalised VDOM fast particle drive for NBI injected ions as a function of Λ_0 , for a case with a circular flux surface and $\epsilon = r/R_0 = 0.1$. The region between the two red lines is where a positive drive for VDOM can occur.

Fig. 4: Normalized VDOM fast particle drive λ_h' for p=1 (see Eq. (7)), obtained with a distribution functions from PION simulations of a JET sized plasma with $P_{RF}=6MW$. The red solid line corresponds to a high field side ICRF resonance about 30 cm from the magnetic axis, while the blue dashed line corresponds to a low field side resonance with a similar distance from the magnetic axis. In this example λ_h' was evaluated for a flux surface intersecting the midplane at a radius of around 35 cm.

Energetic ions accelerated by ICRF waves tend to pile up with their Λ values around $\Lambda_{IC} = B_0/B_{IC}$, where the magnetic field B_{IC} is defined by $n_{ic}\omega_{ci}(B_{IC}) = \omega_{IC}$. (n_{ic} is the harmonic number of the ICRF resonance, ω_{ci} is the ion cyclotron frequency, and ω_{IC} is the frequency of the injected Ion Cyclotron wave). This means that for ICRF resonances on the high field, a significant fraction of the ions resonating with the ICRF waves are on trapped orbits near the trapped-passing boundary. On the other hand, for low field side resonances the ions resonating with ICRF are typically much farther away from the trapped passing boundary. It turns out that the closeness to the trapped-passing boundary plays a crucial role for the potential of ICRF accelerated ions to drive VDOMs. To a large extent, because of the structure of $|Y|^2/h_0$ term, the drive of the VDOM by ICRF accelerated ions requires that the energetic ions are not too far away from the trapped-passing boundary. This is clearly seen in full simulations of $\lambda_h^{'}$. To illustrate this, the PION code (augmented with a package for better assessing the anisotropy of the distribution function [25]) has been run for typical parameters of a JET sized plasma with 6MW of ICRF power. Two cases have been analysed. In the first case, the ICRF resonance was about 30 cm to the low field side of the magnetic axis, and in the second case around 30 cm to the high field side (as measured in the mid-plane). The contributions to the normalized fast particle drive λ'_h . For the two cases from a flux surface with a radius of approximately 35 cm in the midplane is shown in Fig. 4. As can be seen, ICRF accelerated ions only has potential to drive the VDOM for high field side resonances.

6. NUMERICAL SIMULATIONS OF VERTICAL DISPLACEMENT OSCILLATORY MODES

The analytic theory of VDOM, developed based on simplified straight-tokamak equilibria and reviewed in Secs 2-5, have been confirmed by numerical simulations in realistic tokamak geometry using the NIMROD code [26]. NIMROD [27] is a 3D, initial value, extended-MHD, linear and nonlinear code, that allows for the treatment of a low-density, low-temperature "halo" plasma region of varying thickness between the last-closed-flux-surface and the plasma wall. This is particularly important for the study of VDOM, which, as we have pointed out, are external plasma modes that rely on the interaction between the shifting plasma current and the induced currents on the plasma wall. In the first part of this Section, we discuss how VDOM can be recognized in simulations of JET plasmas, using a version of NIMROD that does not include the kinetic-MHD module for the fast particle drive.

We present original NIMROD simulations of JET discharges produced during the 2023 DT3 campaign, where high-frequency n=0 fluctuations where observed, as reported in [7].

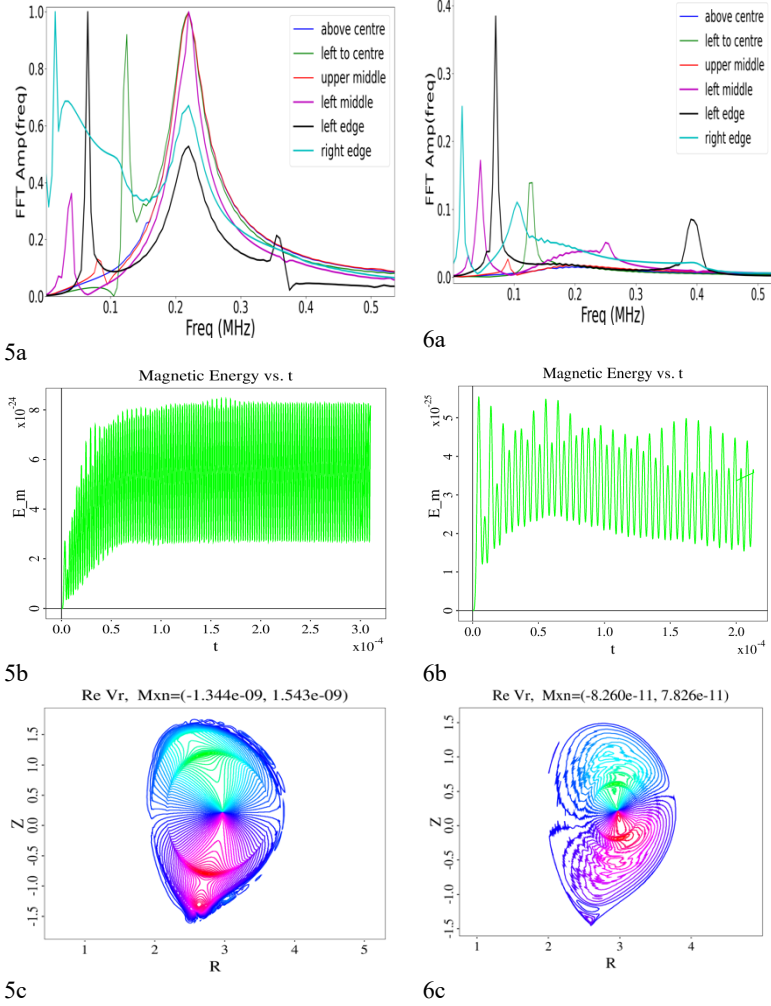


Fig. 5: Plasma normal mode corresponding to a VDOM. (a) FFT spectra of the plasma response taken at different positions in the plasma; (b) magnetic energy as a function of time after forced oscillations at frequency $\omega_{forced} = 217 \ kHz$; (c) contour plots of the perturbed plasma flow orthogonal to equilibrium flux surfaces.

Fig. 6: Alfvén quasi-mode interacting with the Alfvén continuum. (a) FFT spectra taken at different plasma positions; (b) magnetic energy as function of time after forced oscillations at frequency $\omega_{forced} = 217 \ kHz$; (c) contour plots of the perturbed plasma flow normal to equilibrium flux surfaces.

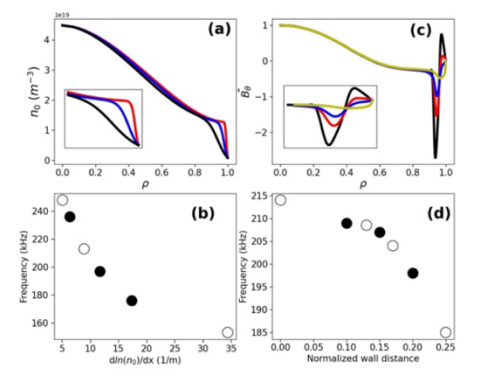


Fig. 7: NIMROD simulation of JET shot #104408. (a) Equilibrium density profile for the pedestal scan; (b) Radial profile of the n=0 perturbed poloidal magnetic field; (c) n=0 mode frequency vs pedestal density gradient and (d) vs normalized wall distance.

These experimental observations are particularly relevant, because they indicate for the first time that n=0 modes are clearly driven by fusion alpha particles and not by other types of energetic particles produced by either NBI or ICRF. In the second part of this Section, we present preliminary numerical results of n=0 VDOM driven unstable by fast particles having a bump on-tail distribution function, based on a newly developed kinetic-MHD module implemented in NIMROD.

If the fast particle drive is absent, the question that comes to mind: is how to recognize a stable normal mode with an initial value code? After all, given an initial condition representing a generic perturbation, all sorts of stable normal modes as well as continuum Alfvén quasimodes are excited. If a particular normal mode is to be identified, it must be driven somehow to finite amplitude, so that its perturbed fields dominate over the sea of all the other stable plasma fluctuations. The procedure that we follow was clearly explained in Ref. [26]. In essence, after an initial transient, Fast Fourier Transform (FFT) is employed to analyse the temporal behaviour of the plasma response in specified positions inside the plasma. Normally, the FFT exhibits one or more peaks at particular frequency values. However, the FFT spectrum may be different for different plasma positions.

Examples of FFT spectra are shown in Figs. 5 and 6, using a realistic JET equilibrium. When a normal mode is present, FFT spectra coming from different parts of the plasma peak and are synchronized around a particular frequency, as shown in Fig. 5a. We then used a forced oscillator mimicking the injection of a wave from an external antenna to resonate with the peak frequency, $\omega_{forced} = 217 \text{ kHz}$. The magnetic energy grows to finite amplitude and then saturates, as shown in Fig. 5c. By contrast, when the VDOM is absent, the FFT spectra are not synchronized, as shown if Fig. 6a. Using forced oscillations at any of the peaks shown in Fig. 6a will not lead to a growing and saturated magnetic energy, as shown in Fig. 6b. The contour plots of the normal perturbed flow are not as neat as those corresponding to a normal mode, as shown in Fig. 6c, and they change in time. Having elucidated how we can identify the presence, frequency and mode structure of a VDOM in numerical simulations even in the absence of the fast particle drive, we now turn to simulations of VDOM in JET discharge #104408 from the last DT3 campaign [7, 8]. With an ideal conducting wall placed at the separatrix, NIMROD finds a mode

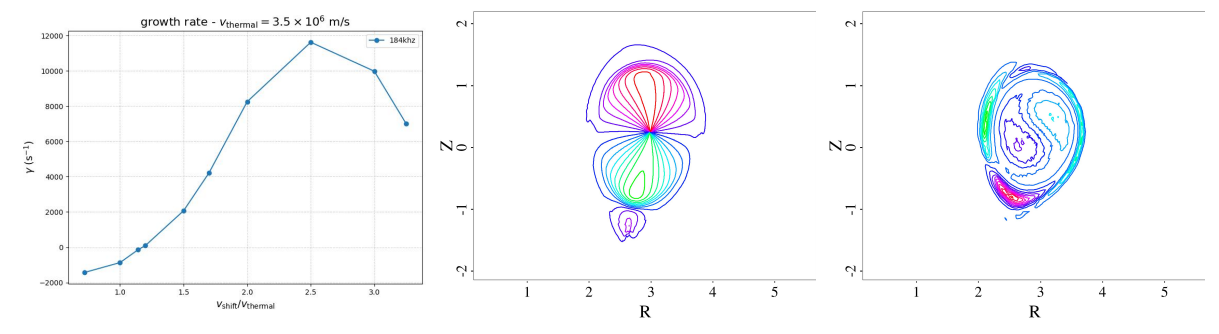


Fig. 8: Plot of the linear growth rate as function of the shifted Maxwellian bump-on-tail (with v_{therm} =3.5e6m/2).

Fig. 9: Contours of the normal component of the plasma flow velocity.

Fig. 10: Contours of the fast particle density, n_h .

which can be either a GAE or a VDOM. To distinguish between the two, we have performed scans in the density pedestal gradient as well as in the plasma-wall distance. The results are shown in Fig. 7. As the steepness of the pedestal density gradient increases, the frequency is observed to decrease. As the wall is moved away from the separatrix, the frequency of the n=0 mode decreases. A realistic value for the wall-separatrix normalised distance in the relevant JET experiments is 0.25, for which NIMROD finds the frequency $\omega = 185$ kHz. These results are in fair agreement with experimental observations and lend support to the interpretation of the mode at JET as a VDOM. A more detailed comparison and analysis is left for a future publication.

Finally, we present preliminary numerical results of n=0 VDOM driven unstable by fast particles having a bump-on-tail distribution function. We use the hybrid kinetic-MHD module in NIMROD [28] to perform linear simulations of VDOMs excited by energetic ions. The module adopts a Particle-in-cell method and the δ f method to linearly push particles and reconstruct the perturbed fast particle distribution function, which is then used to calculate the fast particle pressure tensor within a standard hybrid kinetic-MHD approach. For this VDOM study, the energetic particle module has been modified to use a Maxwellian bump-on-tail distribution function parameterized by its Gaussian width, v_{thermal} , and displacement in parallel velocity of the bump-on-tail, v_{shift} :

$$F_h = C v_{therm}^{-3} \exp\left(-\frac{p_{\varphi}}{\psi_n} - \frac{\left(v_{\parallel} + v_{shift}\right)^2 + v_{\perp}^2}{v_{therm}^2}\right)$$
(7)

where P_{φ} is the toroidal canonical momentum, ψ_n is one-quarter of the total magnetic flux, and C is a normalization constant that ensures a prescribed value of the fast particle beta, β_h . For the simulations reported here, we have chosen $\beta_h = 0.01\beta_{MHD}$. As an initial demonstration of energetic particle excitation of the VDOM, we start with JET shot #102371, which was studied in [26]. These linear hybrid kinetic-MHD simulations use 2M particles and similar NIMROD parameters [26]. Unlike the stable oscillations demonstrated in [26], these simulations show linear destabilization of the VDOM by energetic particles. The linear modes are identified as VDOM by their mode structure and oscillation frequency of 184kHz, in agreement with the observations of [26]. Figure 8 shows a plot of the linear growth as function of $v_{\text{shift}}/v_{\text{therm}}$. The scan shows a minimum shift is necessary to bring the distribution into resonance, overcome the damping of the background plasma and excite the VDOM. As v_{shift} increases, a maximum growth rate occurs when the VDOM resonance (at $\omega = 184\text{kHz}$) aligns with the maximum gradient, $\partial F_h/\partial v$. The growth rate decreases as the bump-on-tail moves away from the VDOM resonance. Figure 9 shows the component of the plasma flow velocity, V_n ; the m=1 up-down parity in this contour plot is indicative of the VDOM. Also, the fast particle density, n_h , shown in Fig. 10, exhibits an m=1 structure in the core but shifted in poloidal phase with respect to V_n . The m=1 core is accompanied by an m=2 structure towards the edge. Note that these contours are snapshots in time and evolve over the VDOM period.

7. CONCLUSIONS

In this article, an overview on the present state-of-the-art on n=0 Vertical Displacement Oscillatory Modes has been presented. This theory may help with the interpretation of experimental observations of n=0 modes observed in recent tokamak experiments. VDOM are driven unstable by fast ions but are also closely associated with vertical displacements that can evolve into VDE and disruptions. We have pointed out that n=0 modes treated within the framework of ideal-MHD are singular at the magnetic X-points of the divertor separatrix. Resolving the

singularity by consideration of resistive effects reveals the formation of current sheets localized near the X-points and extending along the magnetic separatrix. The impact of these current sheets on the stability and turbulent behaviour of the plasma edge, and more in general, a study of 3D magnetic turbulence at the plasma edge in the presence of saturated n=0 mode structures and zonal flows, is a natural continuation of this line of research.

ACKNOWLEDGEMENTS

We would like to thank JET collaborators, and in particular S. Sharapov, J. Oliver and M. Fitzgerald, for providing information and equilibrium reconstruction of interesting JET discharges where n=0 modes have been observed. We also acknowledge useful discussions with M. Podestà and with M. Dreval.

REFERENCES

- [1] Barberis, T., Porcelli, F. and A. Yolbarsop, Fast-ion-driven vertical modes in magnetically confined toroidal plasmas. Nuclear Fusion, 2022. **62**(6).
- [2] Barberis, T., Yolbarsop, A. and Porcelli, F., Vertical displacement oscillatory modes in tokamak plasmas. Journal of Plasma Physics, 2022. 88(5).
- [3] Porcelli, F., Barberis, T. and Yolbarsop, A., Vertical displacements close to ideal-MHD marginal stability in tokamak plasmas, Fundamental Plasma Physics, 2023. 5.
- [4] Yolbarsop, A., et al., Axisymmetric oscillatory modes in cylindrical magnetized plasma bounded by a conducting wall. Physics Letters, Section A: General, Atomic and Solid State Physics, 2023. 479.
- [5] Oliver, H.J.C., et al., Axisymmetric global Alfvén eigenmodes within the ellipticity-induced frequency gap in the Joint European Torus. Physics of Plasmas, 2017. **24**(12).
- [6] Kiptily, V.G., et al., Evidence for Alfvén eigenmodes driven by alpha particles in D-3He fusion experiments on JET, Nuclear Fusion, 2021. **61**(11).
- [7] Oliver, H.J.C. et al, Axisymmetric eigenmodes excited by alpha particle energy gradients in JET D-T plasmas, submitted to Phys. Rev. Lett., July 2025.
- [8] Sharapov, S., et al, Fusion Alpha-Particle-Driven Alfvén Eigenmodes in JET D-T Plasmas: Experiments and Theory, in IAEA FEC2025 Conference, Chengdu, 13-18 October 2025; paper 3056.
- [9] Dreval, K. (KIPT), Podestà, M. (EPFL) and Sharapov, S. (UKAEA), personal communication, 2025.
- [10] Yolbarsop, A., Porcelli, F. and Fitzpatrick, R., *Impact of magnetic X-points on the vertical stability of tokamak plasmas*. Nuclear Fusion, 2021. **61**(11).
- [11] Fu, G.Y., Energetic-particle-induced geodesic acoustic mode. Physical Review Letters, 2008. 101(18).
- [12] Villard, L. and Vaclavik, J., Alfvén frequency modes and global Alfvén eigenmodes. Nucl Fusion, 1997. 37(3): p. 351.
- [13] Fitzpatrick, R., A simple ideal magnetohydrodynamical model of vertical disruption events in tokamaks. Physics of Plasmas, 2009. 16(1).
- [14] Porcelli, F. and Yolbarsop, A., Analytic equilibrium of "straight tokamak" plasma bounded by a magnetic separatrix. Physics of Plasmas, 2019. **26**(5).
- [15] Yolbarsop, A., et al., Analytic theory of ideal-MHD vertical displacements in tokamak plasmas. Plasma Physics and Controlled Fusion, 2022. **64**(10).
- [16] Laval, G., R. Pellat, and J.S. Soule, *Hydromagnetic stability of a current-carrying pinch with noncircular cross section*. Physics of Fluids, 1974. **17**(4): p. 835-845.
- [17] Wesson, J.A., Tokamaks. 2004, Oxford: Clarendon.
- [18] Banerjee, D., et al., Linear NIMROD simulations of n = 0 modes for straight tokamak configuration and comparison with analytic results. Physics of Plasmas, 2024. **31**(2).
- [19] Lingertat, J., et al, Studies of giant ELM interaction with the divertor target in JET. J. Nucl. Materials, 1997. **241-243**: p. 402-407.
- [20] Solano, E.R., Axisymmetric oscillations at L-H transitions in JET: M-mode. Nucl. Fusion, 2016. 57: p. 022021.
- [21] Krebs, I., et al., Axisymmetric simulations of vertical displacement events in tokamaks: A benchmark of M3D-C1, NIMROD, and JOREK. Physics of Plasmas, 2020. 27(2).
- [22] Porcelli, F., et al., Solution of the drift-kinetic equation for global plasma modes and finite particle orbit widths. Physics of Plasmas, 1994. 1(3): p. 470-480.
- [23] Barberis, T. and F. Porcelli, *Velocity-space distribution function of fast ions in a sawtoothing plasma*. Plasma Physics and Controlled Fusion, 2024. **66**(7).
- [24] Van Zeeland, M.A., et al., Beam modulation and bump-on-tail effects on Alfvén eigenmode stability in DIII-D. Nuclear Fusion, 2021. 61(6).
- [25] Eriksson, L.-G., and Porcelli, F., On the drive of $n_{\varphi} = 0$ modes by ICRF accelerated ions in a tokamak. Nucl. Fusion, 2025. **65**: p. 092005.
- [26] Barberis, T., et al., Simulations of vertical displacement oscillatory modes and global Alfvén Eigenmodes in JET geometry. Nuclear Fusion, 2024. **64**(12).
- [27] Sovinec, C.R., et al., *Nonlinear magnetohydrodynamics simulation using high-order finite elements*. Journal of Computational Physics, 2004. **195**(1): p. 355-386.
- [28] Kim, C.C., and the NIMROD team, *Impact of velocity space distribution on hybrid kinetic-MHD simulation of the (1,1) mode.* Phys. Plasmaa, 2008. **15**: p. 072507.